Published in final edited form as:
J Mol Cell Cardiol. 2014 February ; 67: 112–125. doi:10.1016/j.yjmcc.2013.12.013.

Class I HDACs Regulate Angiotensin II-Dependent Cardiac Fibrosis via Fibroblasts and Circulating Fibrocytes

Sarah M. Williams[1], **Lucy Golden-Mason**[2], **Bradley S. Ferguson**[1], **Katherine B. Douglas**[1], **Maria A. Cavasin**[1], **Kim Demos-Davies**[1], **Michael E. Yeager**[3], **Kurt R. Stenmark**[3], and **Timothy A. McKinsey**[1,#]

[1]Department of Medicine, Division of Cardiology, University of Colorado Denver, Aurora, CO

[2]Division of Gastroenterology and Hepatology, University of Colorado Denver, Aurora, CO

[3]Department of Pediatrics, Division of Pulmonary and Critical Care Medicine, University of Colorado Denver, Aurora, CO

Abstract

Fibrosis, which is defined as excessive accumulation of fibrous connective tissue, contributes to the pathogenesis of numerous diseases involving diverse organ systems. Cardiac fibrosis predisposes individuals to myocardial ischemia, arrhythmias and sudden death, and is commonly associated with diastolic dysfunction. Histone deacetylase (HDAC) inhibitors block cardiac fibrosis in pre-clinical models of heart failure. However, which HDAC isoforms govern cardiac fibrosis, and the mechanisms by which they do so, remains unclear. Here, we show that selective inhibition of class I HDACs potently suppresses angiotensin II (Ang II)-mediated cardiac fibrosis by targeting two key effector cell populations, cardiac fibroblasts and bone marrow-derived fibrocytes. Class I HDAC inhibition blocks cardiac fibroblast cell cycle progression through derepression of the genes encoding the cyclin-dependent kinase (CDK) inhibitors, p15 and p57. In contrast, class I HDAC inhibitors block agonist-dependent differentiation of fibrocytes through a mechanism involving repression of ERK1/2 signaling. These findings define novel roles for class I HDACs in the control of pathological cardiac fibrosis. Furthermore, since fibrocytes have been implicated in the pathogenesis of a variety of human diseases, including heart, lung and kidney failure, our results suggest broad utility for isoform-selective HDAC inhibitors as anti-fibrotic agents that function, in part, by targeting these circulating mesenchymal cells.

Keywords

Histone deacetylase; fibroblast; fibrocyte; fibrosis

[#]Address correspondence to TAM: T. A. McKinsey, Tel: 303-724-5476, Fax: 303-724-5450, timothy.mckinsey@ucdenver.edu.

Disclosures

No conflicts of interest exist for the authors.

1. Introduction

Fibrosis is characterized by excessive accumulation of extracellular matrix (ECM) proteins in response to chronic stress and injury. Fibrosis contributes to the pathogenesis of a variety of chronic diseases, including heart failure, renal failure and pulmonary hypertension, and has been estimated to play a causal role in nearly 45 percent of deaths in the developed world [1]. Despite the well-recognized link between fibrosis and organ dysfunction, there are currently no FDA-approved therapies that specifically target the fibrogenic process [2].

Fibrosis plays a critical role in cardiac remodeling, which refers to the changes in heart structure and function that occur in response to pathological stress such as long-standing hypertension and myocardial infarction [3]. Remodeling involves cardiomyocyte hypertrophy as well as myocyte death due to apoptosis and necrosis, which can trigger an inflammatory response that culminates in activation of cardiac fibroblasts [4, 5]. Activated cardiac fibroblasts proliferate, migrate and upregulate genes that encode ECM proteins, including collagen I and collagen III, which have been estimated to make up 80% and 10% of total collagen protein in the heart, respectively (6). Cardiac fibroblasts can differentiate into myofibroblasts, a cell type with an even greater capacity to synthesize ECM. Fibrosis may be reparative, replacing areas of myocyte loss with a structural scar following infarction, or reactive (also referred to as nonadaptive), which is triggered in the absence of cell death and involves interstitial ECM deposition in response to long-lasting stress [4, 6].

Fibrosis has diverse functional consequences in the heart. For example, fibrosis increases the passive stiffness of the myocardium, resulting in impaired relaxation and diastolic dysfunction [7, 8]. Additionally, fibrosis can lead to disruption of electrical conduction in the heart, causing arrhythmias, and can limit myocyte oxygen availability and thus exacerbate myocardial ischemia [9]. Interstitial fibrosis is also prevalent in patients with genetic hypertrophic cardiomyopathy (HCM) and in pre-clinical models of HCM (10;11), where it has been shown to contribute with diastolic dysfunction (12;13). Components of the renin-angiotensin-aldosterone system (RAAS) play critical roles in the control of cardiac fibrosis [2, 4, 5]. For example, angiotensin II (Ang II) is a key stimulus for cardiac fibrosis, and clinical trials have shown that angiotensin receptor blockade with losartan causes regression of cardiac fibrosis and improves diastolic function independently of reducing blood pressure in patients with hypertensive heart disease [10, 11]. However, losartan fails to reduce fibrosis in many patients [11], highlighting the need for alternative anti-fibrotic strategies for the heart.

Cardiac fibroblasts have long been viewed as the major producers of ECM during the fibrotic process. However, recent studies have revealed an important role for a population of bone marrow-derived cells, termed fibrocytes, in the control of cardiac fibrosis. Fibrocytes have features of both monocytes and fibroblasts, and are able to adopt a mesenchymal phenotype and contribute to tissue remodeling in response to pathological stress [12–14]. Studies by the Entman lab have demonstrated that age-related cardiac fibrosis and diastolic dysfunction coincide with accumulation of fibrocytes in ventricular interstitial space [15]. Additional studies in mice have demonstrated roles for fibrocytes in Ang II-meditated cardiac fibrosis [16–18], and in fibrosis due to intermittent ischemia [19]. More recently,

patients with hypertensive heart disease were found to have elevated levels of circulating, activated fibrocytes, and fibrocyte numbers correlated with disease severity [20].

Small molecule inhibitors of histone deacetylases (HDACs) have been shown to be efficacious in rodent models of heart failure, blocking pathological cardiac hypertrophy and fibrosis and improving cardiac function [21]. HDACs catalyze removal of acetyl groups from lysine residues in a variety of proteins. There 18 mammalian HDACs that are encoded by distinct genes and are grouped into four classes: class I HDACs (1, 2, 3 and 8), class II HDACs (4, 5, 6, 7, 9 and 10), class III HDACs (SirT 1 – 7) and class IV (HDAC11) [22]. Class I, II and IV HDACs are zinc-dependent enzymes, while class III HDACs, which are also known as sirtuins, require nicotinamide adenine dinucleotide (NAD+) for catalytic activity. “Pan” inhibitors of zinc-dependent HDACs block cardiac fibrosis [23–26]. However, the roles of specific HDAC isoforms in the control of cardiac fibrosis, and the mechanism(s) by which HDACs control the fibrotic process, remain unclear. Here, we demonstrate that selective inhibition of class I HDACs potently blocks cardiac fibrosis in a pre-clinical mouse model of cardiac stress. Class I HDAC inhibition does not block pro-fibrotic inflammation in the heart. Instead, *in vitro* data suggest that the mechanism by which class I HDAC inhibitors block cardiac fibrosis involves suppression of cardiac fibroblast activation and inhibition of the differentiation of fibrocyte precursors into mature, collagen-producing fibrocytes. These findings define novel functions for class I HDACs in the control of cardiac fibrosis, and suggest generalizable translational potential for isoform-selective HDAC inhibitors for the treatment of pathological organ fibrosis by targeting bone marrow-derived fibrocytes.

2. Materials and methods

2.1 Experimental animals

Experiments were conducted in accordance with the National Institutes Health ‘Guide for the Care and Use of Laboratory Animals’, and were approved by the Institutional Animal Care and Use Committee at the University of Colorado Denver. Ten week-old male C57Bl/6J mice (Jackson Labs) were infused with 1.5 ug/kg/min Ang II (Bachem) for three days or two weeks using osmotic mini-pumps (Alzet). For the two-week studies, beginning at the time of pump implantation, mice were given daily intraperitoneal (IP) injections of either vehicle (50:50 DMSO:PEG-300), scriptaid, DPAH or a tubastatin A; MGCD0103, a slow acting benzamide with a long half-life, was administered every other day. All HDAC inhibitors were dosed at 10 mg/kg. For the three day studies, MGCD0103 was administered every second day beginning 18 hours prior to pump implantation. Animals were sacrificed 20 hours following the final administration of compound, unless otherwise indicated. Hemodynamic data were collected via carotid catheterization (Scisense) with animals anesthetized using 2% isoflurane.

2.2 Tissue procurement and processing

Mice were sacrificed by exsanguination and hearts were immediately excised and perfused with ice-cold saline. Left ventricle (LV) was dissected from right ventricle (RV) and sectioned at the papillary muscles; the lower half of the LV was flash frozen for biochemical

and gene expression analyses, while the upper half of the LV was fixed in paraformaldehyde and transferred to 70% ethanol for storage prior to placement in a paraffin block. Total RNA from LVs was isolated using Trizol (Sigma) and LV protein extracts were prepared in PBS containing 300 mM NaCl, 0.5% Triton-X-100 and protease and phosphatase inhibitors (Thermo Scientific).

For histological analysis, sectioned tissue was rehydrated and collagen was stained using picrosirus red dye (Chromaview, Richard-Allen Scientific). All histological analyses were carried out in a blinded manner using an Axiovert 200 inverted microscope with a digital camera equipped with AxioVision imaging software (Zeiss, Germany). Quantification of picrosirius red staining was completed by determining the average stained pixels^2 per total pixels^2 in images of the LV (18 images used per animal).

2.3 Flow cytometry

A mouse LV digestion method was developed based on previously published data [27]. Briefly, atria were removed and LVs and were manually sliced into several smaller pieces in Hank's Buffered Salt Solution (HBSS) containing 30 mM taurine/10 mM HEPES, and then placed in HBSS/30 mM taurine/10 mM HEPES + 0.1% collagenase II (Worthington) + 0.5 ug/ml DNase (Sigma) and incubated at 37°C for 5 minutes. After incubation, tissue was manually disrupted by pipetting; between incubation steps the digestion buffer was removed and the cells in suspension were placed into ice cold stop buffer (HBSS/30 mM taurine/10 mM HEPES + 20% fetal bovine serum [FBS]). Cells were filtered through a 70 μm filter and washed twice in HBSS prior to staining for analysis using a BS Cantos II flow cytometer (BD Biosciences). Cells were pelleted and resuspended in FACS wash buffer (PBS with 1% BSA and 0.1% sodium azide) containing a 1:100 dilution of each of the fluorescently-conjugated antibodies, including anti-CD45-V500 (BD Biosciences), anti-CD11b-APC (eBioscience), anti-Ly6G-APC Cy7 (BD Biosciences), anti-CD34-PE (BD Biosciences) and anti-F4/80-PerCp Cy5.5 (eBioscience); surface staining was completed for 20 minutes at 4°C. Cells were washed prior to resuspension for FACS analysis if only surface labels were required. Intracellular staining was performed after washing and fixing surface stained cells. Cells were fixed and permeabilized in Fix/Perm Buffer (Biolegend) before staining with intracellular markers of interest (collagen I [Rockland] used at 1:100 and αSMA [Sigma] used at 1:250) in Permeabilization Buffer (Biolegend). The anti-collagen I antibody was conjugated to biotin and detected with fluorochrome-conjugated streptavidin (BD Biosciences). Cells stained for intracellular antigens were not labeled with anti-Ly6G or anti-F4/80.

Blood was collected in the presence of 500 mM EDTA from the vena cava of mice at the time of sacrifice. Surface antigens were labeled with fluorochrome-conjugated antibodies, as listed above. Red blood cells were osmotically lysed with Red Blood Cell Lysis Buffer (BD Biosciences). Cells were fixed in Fix/Perm buffer (Biolegend) for 1 hour before washing and labeling. Antibodies were used at the concentations described above, except for anti-αSMA-FITC (Sigma), which was used at 1:100. For all flow cytometry studies, data were collected and visualized using FACSDiva software (BD Biosciences).

2.4 Adult and neonatal cardiac fibroblast preparation

Neonatal rat ventricular fibroblasts (NRVFs) were isolated from myocyte preparations from Sprague-Dawley rats pups (post-partum 1–2 days), as previously described [28]. Adult rat ventricular fibroblasts (ARVFs) were collected by the Langendorff-perfusion method from Sprague-Dawley rats [28]. Both NRVFs and ARVFs were cultured in DMEM with 20% FBS containing penicillin (100 U/ml), streptomycin (100 U/ml) and L-glutamine (29.2 μg/ml) (PSG) cells were used at passage two for all experiments. The degree of α-smooth muscle actin protein expression in passage two ARVFs in shown in sFig. 1. All cell culture supplies were purchased from Cellgro (Mediatech, Inc), unless otherwise noted.

2.5 HDAC activity assays

HDAC activity assays were completed as previously reported [28]. Each HDAC substrate was based on ε-N-acylated lysine, derivatized on the carboxyl group with amino methylcoumarin (AMC) [29]. Subsequent to deacylation by HDACs, trypsin was used to release AMC, resulting in a significant increase in fluorescence. Tissue extracts were prepared in PBS (pH 7.4) containing 0.5% Triton X-100, 300 mM NaCl and protease/phosphatase inhibitor cocktail (Thermo Fisher) using a Bullet Blender homogenizer (Next Advance). Tissue extracts were diluted into PBS buffer in 100 μL total volumes in a 96-well plate (60 μg ventricular protein/well). Substrates were added (5 μL of 1 mM DMSO stock solutions), and the plates were returned to the 37°C incubator for 2 – 3 hours. Finally, developer/stop solution was added (50 μL per well of PBS with 1.5% Triton X-100, 3 μM TSA, and 0.75 mg/mL trypsin), with another 20 minute incubation at 37°C. AMC fluorescence was measured using a BioTek Synergy 2 plate reader, with excitation and emission filters of 360 nm and 460 nm, respectively (each with bandwidth 40 nm), along with a 400 nm dichroic top mirror. Background signals from buffer blanks were subtracted, and data were normalized as needed using appropriate controls.

For determining HDAC activity in living cells, ARVFs were seeded on 96-well plates (10,000 cells/well). Cells were allowed to adhere overnight and were subsequently cultured in serum-free DMEM containing PSG and Neutridoma-SP (0.1%; Roche). For concentration-response determination, cells were dosed with increasing semi-log scale concentrations of HDAC inhibitors for 24 hours prior to addition of cell-permeable fluorescent HDAC substrates [29]. After two hours, stop buffer (PBS+1.5 Triton-X, 3 mM TSA 0.75ug/ul) was added to each well and incubated for 20 minutes at 37°C. Deacetylated substrates were susceptible to trypsin cleavage, which resulted in increased fluorescence. GraphPad Prism was used to calculate the IC_{50} values for each compound.

2.6 Cell cycle analysis

NRVFs were passaged at a 1:6 ratio 24 hours prior to serum deprivation in full serum media, and refreshed with serum starvation medium (DMEM containing 0.1% Nutridoma Supplement (Roche) and PSG for 18 hours in order to synchronize the cells in G_0/G_1. Cells were then refed with medium containing 20% FBS in the presence of either vehicle (DMSO) or HDAC inhibitors. Samples of cells were collected after 18 hours of serum starvation as 0 hr controls. Cell cycle analysis was completed by washing NRVFs in cold PBS followed by a brief 1 minute trypsinization. Cells were washed in PBS and pelleted cells were fixed with

ice cold 70% ethanol. Prior to flow cytometry analysis, samples were placed on ice for 30 minutes and washed once with cold PBS. An equal amount of staining solution (50 ug/ml propium iodide [Sigma] and 100 ug/ml RNase [Qiagen]) was added to each sample to stain DNA. Samples were processed with a BD Cantos II Flow Cytometer (5000 FSC/SSC-gated cells were captured per sample).

2.7 Immunoblotting and quantitative PCR

Extracts were prepared in PBS (pH 7.4) containing 0.5% Triton X-100, 300 mM NaCl and protease/phosphatase inhibitor cocktail (Thermo Fisher) using a Bullet Blender homogenizer (Next Advance). Protein concentrations were determined using a BCA Protein Assay Kit (Pierce). Proteins were resolved by SDS-PAGE, transferred to nitrocellulose membranes (BioRad) and probed with antibodies for α-tubulin (Santa Cruz Biotechnology, sc-23948), phospho-Rb (Cell Signaling Technology, cs-9308, S807/811), p15 (Cell Signaling Technology, cs-4822), cyclin D1 (Cell Signaling Technology, cs-2926), p21 (Abcam, GR48008-1), p27 (Cell Signaling Technology, cs-3686), phospho-STAT6 (Cell Signaling Technology, cs-9361, Y641), phospho-ERK1/2 (Cell Signaling Technology, cs-4376, T202/Y204), phospho-ELK1 (Cell Signaling Technology, cs-9186, S383), phospho-JNK (Cell Signaling Technology, cs-4668, T183/Y185), phospho-p38 (Cell Signaling Technology, cs-4631, T180/Y182) or GAPDH (Santa Cruz Biotechnology, sc-20357). HRP-conjugated secondary antibodies (Southern Biotech) were used at a concentration of 1:2000.

For qPCR, total RNA was harvested using TRI Reagent™ (Life Technologies) 48 hours after treatment. All RNA samples were diluted to 100 ng/μl, and 5 μl (500 ng) of RNA was converted to cDNA using the Verso™ cDNA Synthesis Kit (Thermo Scientific). Quantitative PCR (qPCR) was performed using Absolute™ QPCR SYBR Green ROX mix (Thermo Scientific) on a StepOne qPCR instrument (Applied Biosystems). PCR primers for MCP-1, p15, p16, p18, p19, p57 and 18S are shown in Table S1. All qPCR primers were optimized for a slope between −3.1 and −3.6, >90% efficiency, R^2 >0.98, and a single melt curve. Relative transcript levels were determined by measuring Ct values off of a standard curve made from serial dilutions of pooled cDNA.

2.8 In vitro fibrocyte differentiation assay

Human cells were collected from healthy volunteers after informed consent was obtained under Colorado Multiple Institutional Review Board (COMIRB) protocol 13–1700. For peripheral blood mononuclear cell isoloation, red blood cells were lysed using Red Blood Cell Lysis Buffer (BD Biosciences), and cells were washed in PBS containing 0.1% FBS two times prior to plating in DMEM containing 20% FBS and PSG. After 5 days of culture, adherent cells were cultured in serum-free medium (DMEM, 10 mM HEPES, PSG, non-essential amino acids and 0.1% Neuridoma-SP) in the absence or presence of IL-4 (10 ng/ml; PeproTech) and Il-13 (10 ng/ml; PeproTech). Cells were differentiated in the presence of vehicle (DMSO), MGCD (250 nM), and SAP (1 μg/ml; Calbiochem). Samples of cells before and after stimulation were collected and used for flow cytometric anaylsis. Cells were fixed with Fixation/Permeabilization buffer (Biolegend) and incubated with biotinylated anti-Col I (Rockland) followed by PerCP labeled strepatavidin. Pooled IgG controls and unstained samples were used to set gates for flow cytometry.

2.9 Statistical analysis

Analysis was completed by ANOVA followed by post-hoc testing (Tukey's test was used for post-hoc analysis unless otherwise noted); statistical analysis was completed using GraphPad Prism software. Statisitcal significance (α defined as 0.05) is reported as applicable.

3. Results

3.1 Class I HDAC-selective inhibition blocks cardiac fibrosis

To assess the role of specific HDAC isoforms in the control of cardiac fibrosis, a panel of isoform-selective HDAC inhibitors was tested for efficacy in a mouse model of Ang II-mediated fibrosis. The small molecule HDAC inhibitors used for this study were scriptaid (a pan-HDAC inhibitor) [30], MGCD0103 (a selective inhibitor of class I HDACs -1, -2 and -3) [31], DPAH (a class IIa HDAC-selective inhibitor) [32], and tubastatin A (Tub A; a selective inhibitor of class IIb HDAC6) [33] (Fig. 1A). Dose-response analyses with cultured cardiac fibroblasts confirmed the selectively profiles of these HDAC inhibitors (sFig. 2). All compounds were delivered via IP injection at 10 mg/kg body weight, with dosing beginning the day of Ang II mini-pump implantation and continuing throughout the two-week period (Fig. 1B). HDAC inhibitor treatment did not significantly alter animal body weight (Fig. 1C) or Ang II-mediated hypertension (Fig. 1D), indicating that the compounds were well tolerated and did not suppress the initiating stimulus for cardiac remodeling. Under these conditions, Ang II did not trigger significant LV hypertrophy or cardiac diastolic or systolic dysfunction (sFig. 3).

Picrosirus red staining of LV sections was performed to assess effects of HDAC inhibitors on cardiac fibrosis. Two weeks of Ang II treatment led to profound cardiac interstitial collagen deposition, which was completely abolished by pan-HDAC inhibition with scriptaid or class I HDAC-selective inhibition with MGCD0103 (Fig. 2A and B; sFig. 4). In contrast, class II HDAC inhibitors failed to block Ang II-mediated cardiac fibrosis. HDAC enzymatic assays with LV homogenates confirmed the specificity of MGCD0103 for class I HDACs (Fig. 2C – E); class I HDACs -1, -2 and -3 were each detected in the mouse LV, and expression of these HDAC isoforms was unaffected by Ang II stimulation (sFig. 5). These data strongly support a role for class I HDACs in the pathogenesis of myocardial fibrosis.

3.2 Class I HDAC inhibition does not reduce Ang II-mediated inflammation in the LV

Inflammation has long been recognized as a key stimulus for the development of cardiac fibrosis, and recent work demonstrated that recruitment of leukocytes to the heart is necessary for cardiac fibrogenesis [16, 18, 19]. Given that HDAC inhibitors exhibit broad anti-inflammatory activity [34, 35], we hypothesized that suppression of cardiac fibrosis by MGCD0103 was due to blockade of Ang II-mediated immune cell recruitment. To address this possibility, flow cytometric analysis was performed with single-cell suspensions of LVs from mice treated with Ang II for three days in the absence or presence of MGCD0103; the three day time point was chosen based on prior studies showing the most dramatic changes in immune cell recruitment and inflammatory signaling shortly after initiation of Ang II

treatment [16, 36]. Consistent with this, total leukocyte ($CD45^+$ cells) numbers were significantly elevated in hearts of mice receiving Ang II (Fig. 3A and B). Surprisingly, however, leukocyte infiltration was not reduced in the animals treated with the class I HDAC inhibitor MGCD0103 (Fig. 3A and B). Furthermore, MGCD0103 also failed to decrease Ang II-mediated recruitment of monocytes/macrophages ($CD45^+CD11b^+Ly6G^-$) and neutrophils ($CD45^+CD11b^+Ly6G^+$) to the heart (Fig. 3C – E). These data suggest that class I HDAC inhibition blocks cardiac fibrosis independently of effects on inflammatory responses.

3.3 Class I HDAC inhibition blocks cardiac fibroblast cell cycle progression

In response to pathogenic stimuli, cardiac fibroblasts proliferate and produce excess amounts of ECM. Experiments were performed to assess the possibility that HDAC inhibitors block cardiac fibrosis by altering these effector cells. To investigate effects of isoform-selective HDAC inhibition on cardiac fibroblast cell cycle progression, cultured neonatal rat ventricular fibroblasts (NRVFs) were synchronized in G_0/G_1 of the cell cycle by serum starvation, and cell cycle progression was reinitiated with FBS in the absence or presence of HDAC inhibitors. Cell cycle progression was assessed by measuring propidium iodide (PI) staining in fixed NRVFs. Initial time course studies with trichostatin A (TSA) revealed that treatment with this pan-HDAC inhibitor blocked NRVFs in G_0/G_1 of the cell cycle (Fig. 4A and B). Subsequent experiments using isoform-selective HDAC inhibitors demonstrated that cardiac fibroblast cell cycle arrest was due to class I HDAC inhibition (Fig. 4C and D). Identical results were obtained with adult rat ventricular fibroblasts (ARVFs), suggesting that class I HDACs serve a generalizable role in the control of cardiac fibroblast proliferation (Fig. 4E). Immunoblotting confirmed that class I HDACs -1, -2 and -3 are expressed in ARVFs (Fig. 4F).

Although several studies have demonstrated that HDAC inhibitors block cell cycle progression in cancer cells [37, 38], this effect has not been previously reported in cardiac fibroblasts. In cancer cells, anti-proliferative effects of HDAC inhibitors involve upregulation of the genes encoding the cyclin-dependent kinase inhibitors p21 and p27. These CDK inhibitors block the action of cyclin-dependent kinase 4/6 (CDK4/6):cyclin D_1 complexes, thereby preventing phosphorylation of retinoblastoma protein (Rb), which is required to stimulate genes to promote the transition from G_1 to the S phase of the cell cycle; other endogenous CDK inhibitors include p15, p16, p18, p19 and p57 (Fig. 5A). Immunoblot analysis revealed that class I HDAC inhibition efficiently blocked stimulus-dependent Rb phosphorylation in cardiac fibroblasts (Fig. 5B). The presence of cyclin D_1 in NRVFs treated with MGCD0103 confirmed that the cells were blocked in the G_1 phase of the cell cycle. Surprisingly, however, p21 and p27 expression levels were unaffected by the HDAC inhibitor (Fig. 5B). A subsequent quantitative PCR survey of other CDK inhibitors revealed that class I HDAC inhibition in cardiac fibroblasts results in selective upregulation of p15 and p57 (Fig. 5C – G); induction of p15 and p57 mRNA expression by MGCD0103 was confirmed using multiple independent cultures of ARVFs (Fig. 5H and I). MGCD0103 also stimulated p15 protein expression (Fig. 5J); we were unable to identify a commercial antibody that efficiently recognizes rat p57 (data not shown). These data suggest that class I

HDAC inhibition blocks cardiac fibroblast proliferation, in part, through suppression of CDK activity via induction of p15 and p57 (Fig. 5K).

3.4 Class I HDAC inhibition blocks differentiation of fibrogenic bone marrow-derived fibrocytes

In addition to cardiac fibroblasts, recent studies have clearly revealed an important role for a population of bone marrow-derived cells, termed fibrocytes, in the control of cardiac fibrosis. Fibrocytes have features of both monocytes and fibroblasts, and are able to adopt a mesenchymal phenotype and contribute to tissue remodeling in response to pathological stress [12–14]. Additional flow cytometric analyses were performed to begin to address whether the mechanism of HDAC inhibitor-meditated suppression of cardiac fibrosis also involves effects on fibrocytes. Fibrocytes are defined by co-expression of CD34 (stem cell marker), CD45 (hematopoietic cell marker), a monocyte markers (e.g., CD11), and either collagen or α-smooth muscle actin (mesenchymal markers) [12]. Consistent with prior studies, mice treated with Ang II had significantly elevated levels of fibrocytes in the heart [16, 36]. Remarkably, class I HDAC inhibition with MGCD0103 completely blocked Ang II-mediated increases in fibrocytes in the heart (Fig. 6A – C), and also decreased circulating levels of fibrocytes (Fig. 6D; sFig. 6); antibody controls confirmed the integrity of the flow cytometry data (sFig. 7). HDAC inhibitor-mediated suppression of fibrocytes did not appear to be due to blockade of recruitment to the heart, since monocytic fibrocyte precursors were equally abundant in hearts of mice treated with Ang II in the absence or presence of MGCD0103 (Fig. 6E and F). Consistent with this, cardiac expression of monocyte chemoattractant protein-1 (MCP-1), which is critical for fibrocyte recruitment to the heart [16], was induced by Ang II despite class I HDAC inhibition (Fig. 6G). MGCD0103 appeared to enhance MCP-1 expression in the LV, and this was also observed in cultured cardiac fibroblasts (sFig. 8). The mechanism underlying the stimulatory effect of MGCD0103 on MCP-1 expression remains unclear. Nonetheless, the data support the notion that class I HDAC inhibition blocks fibrocyte differentiation, rather than recruitment of these cells to the heart.

To begin to address the possibility that HDACs serve a novel role in the control of fibrocyte differentiation, *in vitro* assays were performed with peripheral blood mononuclear cells (PBMCs) isolated from whole human blood. Fibrocyte precursors were allowed to adhere to culture plates for five days in the presence of FBS prior to stimulation with IL-4 and IL-13, which are known to trigger fibrocyte differentiation (Fig. 7A) [39]. Some cells received serum amyloid P (SAP), which has previously been shown to block fibrocyte differentiation [40], and other cells received MGCD0103. Strikingly, MGCD0103 blocked fibrocyte differentiation as effectively as SAP (Fig. 7A and B), suggesting a critical role for class I HDACs in the control of this process.

Extracellular signal-regulated kinase (ERK), p38 and c-Jun N-terminal kinase (JNK), as well as Signal Transducer and Activator of Transcription 6 (STAT6), have all been implicated in the control fibrocyte differentiation [12–14]. Immunoblotting was performed to address whether class I HDAC inhibition suppresses fibrocyte differentiation via alterations of these intracellular effectors. IL-4/IL-13 stimulation of adherent fibrocyte precursors led to

enhanced phosphorylation (activation) of STAT-6, ERK1/2 and JNK; p38 phosphorylation was not increased in stimulated cells (Fig. 7C). Class I HDAC inhibition with MGCD0103 had no effect on the phosphorylation status of STAT6, JNK and p38, but dramatically reduced dual phosphorylation of ERK1/2 on threonine and tyrosine residues, a condition that is necessary and sufficient for activation of the kinase (Fig. 7C). Consistent with this, IL-4/IL-13-mediated phosphorylation of ELK, a downstream substrate of ERK1/2, was significantly reduced in cells treated with the class I HDAC inhibitor. Follow-up studies with PBMCs from six different individuals confirmed that MGCD0103 consistently suppresses ERK1/2 phosphorylation in fibrocyte precursors (Fig. 7D). These data suggest that class I HDAC inhibition blocks fibrocyte differentiation, at least in part, by suppressing ERK signaling.

4. Discussion

The findings of this study establish class I HDACs as key regulators of cardiac fibrosis that serve dual fibrogenic functions by promoting cardiac fibroblast activation and controlling differentiation of bone marrow-derived fibrocytes (Fig. 7D). The critical role for class I HDACs in the control of cardiac fibrosis was defined using a series of isoform-selective inhibitors of HDACs as chemical genetic probes in a pre-clinical model. Whereas pan- and class I HDAC-selective inhibitors efficiently blocked cardiac fibrosis mediated by Ang II, small molecules targeting class IIa and IIb HDACs were ineffective (Fig. 2). Our results suggest a novel application for class I HDAC-selective small molecules for the treatment of fibrotic diseases, including heart failure.

Pan-HDAC inhibitors have been shown to reduce pressure overload-driven interstitial cardiac fibrosis and to reverse pre-established atrial fibrosis and arrthythmic inducibility in Hop transgenic mice [23–26]. However, the molecular basis for the anti-fibrotic actions of HDAC inhibitors has not been addressed. Here, we show that class I HDACs govern proliferation of cardiac fibroblasts (Fig. 4), which make up ~70% of the cells in the heart and serve a major role in ECM production. Class I HDAC inhibition blocks cardiac fibroblasts in the G_0/G_1 phase of the cell cycle via inhibition of Rb phosphorylation (Fig. 5B), which is mediated by CDK and is required to stimulate downstream expression of E2F target genes that drive the G_1-to-S transition. A major mechanism for inhibition of cancer cell proliferation by HDAC inhibitors involves induction of expression of the p21 CDK inhibitor [38, 41–44]. Surprisingly, class I HDAC inhibition failed to stimulate expression of p21 in cardiac fibroblasts (Fig. 5B). Instead, a survey of expression of the six other endogenous CDK inhibitors revealed that class I HDAC inhibition selectively upregulates p15 and p57 (Fig. 5B – J), uncovering a previously unrecognized role for these genes in cardiac fibrosis. The results suggest that one mechanism by which class I HDACs stimulate fibrosis in the heart is by repressing expression of anti-proliferative genes in cardiac fibroblasts, resulting in expansion of the pool of ECM-producing cells in the myocardium in response to stress.

We originally hypothesized that repression of fibrosis by class I HDAC inhibitors would involve suppression of inflammatory triggers, since inflammation has long been known to stimulate fibroblast activation and fibrosis [2, 45], and HDAC inhibitors have well

documented anti-inflammatory activity [46–48]. Surprisingly, however, treatment of mice with MGCD0103 failed to block accumulation of monocytes, macrophages and neutrophils in hearts of Ang II-treated mice (Fig. 3). Instead, class I HDAC inhibitor treatment led to a remarkable reduction in the number of bone marrow-derived fibrocytes in the heart in Ang II treated mice (Fig. 6A – C), and also reduced circulating levels of fibrocytes (Fig. 6D). Class I HDAC inhibition did not decrease recruitment of fibrocyte precursors to the heart (Fig. 6E and F), and, consistent with this, MGCD0103 did not suppress cardiac expression of MCP-1, which has previously been shown to be required for Ang II-mediated migration of fibrocytes to the LV (Fig. 6G) [16]. These data support a role for class I HDACs in the control of fibrocyte differentiation rather than recruitment of these cells to the heart.

A function for class I HDACs in the regulation of fibrocyte differentiation was confirmed using an *in vitro* differentiation assay with human PBMCs. We found that class I HDAC inhibition blocks fibrocyte differentiation as efficiently as SAP (Fig. 7A and B), an Fcγ receptor antagonist that is currently in clinical development for idiopathic pulmonary fibrosis [40]. Compared to cardiac fibroblasts, little is known about the molecular mechanisms that control fibrocyte differentiation and growth. Several receptor agonists have been shown to stimulate fibrocyte differentiation, including TGF-β, ET-1, IL-4 and IL-13 [12–14]; TNFα signaling also appears to be involved [49]. Recently, ERK1/2 was found to be a critical downstream effector of fibrocyte differentiation. Specifically, the prostacyclin analogue treprostinil was shown to block fibrocyte differentiation by triggering cAMP-mediated inhibition of ERK, and this was mimicked by the ERK1/2 inhibitor, UO126 [50]. Rho kinase [51], p38 kinase [52] and STAT transcription factors [39] have also been implicated in the control of fibrocyte differentiation. A survey of pathways known to control fibrocyte differentiation demonstrated that MGCD0103 selectively inhibits activation of ERK1/2 (Fig. 7C and D). The mechanism by which class I HDAC inhibition blocks ERK activation in fibrocytes remains unknown, but could be related to our recent finding that class I HDAC inhibitors suppress ERK signaling in cardiac myocytes by derepressing expression of an ERK-specific phosphatase, termed DUSP5 [53].

HDAC inhibitors have been shown to block fibrosis in diverse organs. We propose that the ability of HDAC inhibitors to suppress fibrocyte differentiation provides a unifying mechanism to explain the broad-spectrum anti-fibrotic actions of this compound class. Indeed, in addition to heart failure, fibrocytes have been implicated in the pathogenesis of numerous diseases that have fibrotic components [13], including rheumatoid arthritis [54], pulmonary fibrosis [55, 56], pulmonary hypertension [57, 58], acute lung injury [59], long term organ rejection [60], chronic kidney disease [61] and liver failure [62].

We cannot rule out the possibility that HDAC inhibitors block cardiac fibrosis through additional mechanisms. For example, expression of the pro-fibrotic mediator, TGF-β, is known to be induced by Ang II [4], and recent studies in models of renal fibrosis have suggested that class I HDAC inhibitors suppress TGF-β expression in the kidney [63]. Future studies will need to address the impact of class I HDAC inhibitors on TGF-β signaling in the heart.

Cardiac fibrosis is a characteristic of numerous pathological conditions, and likely contributes to the pathogenesis of diastolic dysfunction leading to heart failure with preserved ejection fraction (HFpEF), since excess ECM increases myocardial stiffness [64–67]. The urgent need for anti-fibrotic therapeutics for the heart is underscored by the fact that HFpEF affects ~3 million Americans and is steadily increasing in incidence [68, 69]. Our data suggest that isoform-selective HDAC inhibitors hold promise as highly effective anti-fibrotic agents by virtue of their ability to simultaneously target two key fibrogenic effector cell populations, cardiac fibroblasts and circulating fibrocytes. The ability of HDAC inhibitors to block cardiac fibrosis in the face of sustained hypertension (Fig. 1D) reveals that this compound class functions through mechanisms that are distinct from previously tested drugs that target components of the RAAS system, and suggests potential for synergy between HDAC inhibitors and other anti-fibrotic agents. Given the known benefits of blood pressure control in the context of heart failure, combination therapy involving HDAC inhibitors and anti-hypertensive drugs would be obligatory.

In summary, the data presented here suggest potential for class I HDAC-selective inhibitors for the treatment of pathological cardiac fibrosis. MGCD0103 (Mocetinostat) is the small molecule inhibitor that was used to validate class I HDACs as targets for cardiac fibrosis. This and other class I HDAC-selective inhibitors (e.g., Entinostat), are in clinical development for cancer and are well tolerated by humans, highlighting the translational potential of the present findings [70]. Nonetheless, additional pre-clinical optimization is clearly needed before HDAC inhibitors can be advanced into clinical testing in humans with cardiac fibrosis. For example, since MCP-1 has been linked to adverse cardiac remodeling [16, 71], it will be important to address whether the observed increase in MCP-1 expression in hearts and cultured cardiac cells exposed to MGCD0103 (Fig. 6G and sFig. 8) is specific for this compound or is a common effect of all class I HDAC inhibitors. It may be possible to circumvent this issue with newer generations of compounds that selectively inhibit HDAC1, HDAC2 or HDAC3, rather than all three of these class I HDAC isoforms simultaneously [72]. Notwithstanding this uncertainty, isoform-selective HDAC inhibitors clearly hold promise as novel anti-fibrotic agents.

Supplementary Material

Refer to Web version on PubMed Central for supplementary material.

Acknowledgments

We thank J. Mahaffey for ARVF preparation, W. W. Blakeslee for histology, M. K. McKinsey for graphics, A.P. Kozikowski (U. of Illinois Chicago) for Tubastatin A and C.S. Long and P.M. Buttrick for advice and critical reading of the manuscript. S.M.W. was funded by a pre-doctoral fellowship from the NIH/NCRR (TL5TL1RR025778-04). B.S.F. was supported by a postdoctoral fellowship from the American Heart Association (12POST10680000). B.S.F. and K.B.D. received funding from a T32 training grant from the NIH (5T32HL007822-12).

References

1. Wynn TA. Fibrotic disease and the T(H)1/T(H)2 paradigm. Nat Rev Immunol. 2004; 4:583–94. [PubMed: 15286725]

2. Wynn TA, Ramalingam TR. Mechanisms of fibrosis: therapeutic translation for fibrotic disease. Nat Med. 2012; 18:1028–40. [PubMed: 22772564]
3. Berk BC, Fujiwara K, Lehoux S. ECM remodeling in hypertensive heart disease. J Clin Invest. 2007; 117:568–75. [PubMed: 17332884]
4. Brown RD, Ambler SK, Mitchell MD, Long CS. The cardiac fibroblast: therapeutic target in myocardial remodeling and failure. Annu Rev Pharmacol Toxicol. 2005; 45:657–87. [PubMed: 15822192]
5. Porter KE, Turner NA. Cardiac fibroblasts: at the heart of myocardial remodeling. Pharmacol Ther. 2009; 123:255–78. [PubMed: 19460403]
6. Silver MA, Pick R, Brilla CG, Jalil JE, Janicki JS, Weber KT. Reactive and reparative fibrillar collagen remodelling in the hypertrophied rat left ventricle: two experimental models of myocardial fibrosis. Cardiovasc Res. 1990; 24:741–7. [PubMed: 2146020]
7. Brower GL, Gardner JD, Forman MF, Murray DB, Voloshenyuk T, Levick SP, et al. The relationship between myocardial extracellular matrix remodeling and ventricular function. Eur J Cardiothorac Surg. 2006; 30:604–10. [PubMed: 16935520]
8. Moreo A, Ambrosio G, De CB, Pu M, Tran T, Mauri F, et al. Influence of myocardial fibrosis on left ventricular diastolic function: noninvasive assessment by cardiac magnetic resonance and echo. Circ Cardiovasc Imaging. 2009; 2:437–43. [PubMed: 19920041]
9. Sabbah HN, Sharov VG, Lesch M, Goldstein S. Progression of heart failure: a role for interstitial fibrosis. Mol Cell Biochem. 1995; 147:29–34. [PubMed: 7494551]
10. Ciulla MM, Paliotti R, Esposito A, Diez J, Lopez B, Dahlof B, et al. Different effects of antihypertensive therapies based on losartan or atenolol on ultrasound and biochemical markers of myocardial fibrosis: results of a randomized trial. Circulation. 2004; 110:552–7. [PubMed: 15277331]
11. Diez J, Querejeta R, Lopez B, Gonzalez A, Larman M, Martinez Ubago JL. Losartan-dependent regression of myocardial fibrosis is associated with reduction of left ventricular chamber stiffness in hypertensive patients. Circulation. 2002; 105:2512–7. [PubMed: 12034658]
12. Herzog EL, Bucala R. Fibrocytes in health and disease. Exp Hematol. 2010; 38:548–56. [PubMed: 20303382]
13. Peng H, Herzog EL. Fibrocytes: emerging effector cells in chronic inflammation. Curr Opin Pharmacol. 2012; 12:491–6. [PubMed: 22465542]
14. Reilkoff RA, Bucala R, Herzog EL. Fibrocytes: emerging effector cells in chronic inflammation. Nat Rev Immunol. 2011; 11:427–35. [PubMed: 21597472]
15. Cieslik KA, Taffet GE, Carlson S, Hermosillo J, Trial J, Entman ML. Immune-inflammatory dysregulation modulates the incidence of progressive fibrosis and diastolic stiffness in the aging heart. J Mol Cell Cardiol. 2011; 50:248–56. [PubMed: 20974150]
16. Haudek SB, Cheng J, Du J, Wang Y, Hermosillo-Rodriguez J, Trial J, et al. Monocytic fibroblast precursors mediate fibrosis in angiotensin-II-induced cardiac hypertrophy. J Mol Cell Cardiol. 2010; 49:499–507. [PubMed: 20488188]
17. Sopel M, Falkenham A, Oxner A, Ma I, Lee TD, Legare JF. Fibroblast progenitor cells are recruited into the myocardium prior to the development of myocardial fibrosis. Int J Exp Pathol. 2012; 93:115–24. [PubMed: 22225615]
18. Xu J, Lin SC, Chen J, Miao Y, Taffet GE, Entman ML, et al. CCR2 mediates the uptake of bone marrow-derived fibroblast precursors in angiotensin II-induced cardiac fibrosis. Am J Physiol Heart Circ Physiol. 2011; 301:H538–H547. [PubMed: 21572015]
19. Haudek SB, Xia Y, Huebener P, Lee JM, Carlson S, Crawford JR, et al. Bone marrow-derived fibroblast precursors mediate ischemic cardiomyopathy in mice. Proc Natl Acad Sci U S A. 2006; 103:18284–9. [PubMed: 17114286]
20. Keeley EC, Mehrad B, Janardhanan R, Salerno M, Hunter JR, Burdick MM, et al. Elevated circulating fibrocyte levels in patients with hypertensive heart disease. J Hypertens. 2012; 30:1856–61. [PubMed: 22796709]
21. Bush EW, McKinsey TA. Protein acetylation in the cardiorenal axis: the promise of histone deacetylase inhibitors. Circ Res. 2010; 106:272–84. [PubMed: 20133912]

22. Gregoretti IV, Lee YM, Goodson HV. Molecular evolution of the histone deacetylase family: functional implications of phylogenetic analysis. J Mol Biol. 2004; 338:17–31. [PubMed: 15050820]
23. Gallo P, Latronico MV, Gallo P, Grimaldi S, Borgia F, Todaro M, et al. Inhibition of class I histone deacetylase with an apicidin derivative prevents cardiac hypertrophy and failure. Cardiovasc Res. 2008; 80:416–24. [PubMed: 18697792]
24. Kee HJ, Sohn IS, Nam KI, Park JE, Qian YR, Yin Z, et al. Inhibition of histone deacetylation blocks cardiac hypertrophy induced by angiotensin II infusion and aortic banding. Circulation. 2006; 113:51–9. [PubMed: 16380549]
25. Kong Y, Tannous P, Lu G, Berenji K, Rothermel BA, Olson EN, et al. Suppression of class I and II histone deacetylases blunts pressure-overload cardiac hypertrophy. Circulation. 2006; 113:2579–88. [PubMed: 16735673]
26. Liu F, Levin MD, Petrenko NB, Lu MM, Wang T, Yuan LJ, et al. Histone-deacetylase inhibition reverses atrial arrhythmia inducibility and fibrosis in cardiac hypertrophy independent of angiotensin. J Mol Cell Cardiol. 2008; 45:715–23. [PubMed: 18926829]
27. Carlson S, Trial J, Soeller C, Entman ML. Cardiac mesenchymal stem cells contribute to scar formation after myocardial infarction. Cardiovasc Res. 2011; 91:99–107. [PubMed: 21357194]
28. Lemon DD, Horn TR, Cavasin MA, Jeong MY, Haubold KW, Long CS, et al. Cardiac HDAC6 catalytic activity is induced in response to chronic hypertension. J Mol Cell Cardiol. 2011; 51:41–50. [PubMed: 21539845]
29. Heltweg B, Dequiedt F, Marshall BL, Brauch C, Yoshida M, Nishino N, et al. Subtype selective substrates for histone deacetylases. J Med Chem. 2004; 47:5235–43. [PubMed: 15456267]
30. Su GH, Sohn TA, Ryu B, Kern SE. A novel histone deacetylase inhibitor identified by high-throughput transcriptional screening of a compound library. Cancer Res. 2000; 60:3137–42. [PubMed: 10866300]
31. Fournel M, Bonfils C, Hou Y, Yan PT, Trachy-Bourget MC, Kalita A, et al. MGCD0103, a novel isotype-selective histone deacetylase inhibitor, has broad spectrum antitumor activity in vitro and in vivo. Mol Cancer Ther. 2008; 7:759–68. [PubMed: 18413790]
32. Tessier P, Smil DV, Wahhab A, Leit S, Rahil J, Li Z, et al. Diphenylmethylene hydroxamic acids as selective class IIa histone deacetylase inhibitors. Bioorg Med Chem Lett. 2009; 19:5684–8. [PubMed: 19699639]
33. Butler KV, Kalin J, Brochier C, Vistoli G, Langley B, Kozikowski AP. Rational design and simple chemistry yield a superior, neuroprotective HDAC6 inhibitor, tubastatin A. J Am Chem Soc. 2010; 132:10842–6. [PubMed: 20614936]
34. Blanchard F, Chipoy C. Histone deacetylase inhibitors: new drugs for the treatment of inflammatory diseases? Drug Discov Today. 2005; 10:197–204. [PubMed: 15708534]
35. Shakespear MR, Halili MA, Irvine KM, Fairlie DP, Sweet MJ. Histone deacetylases as regulators of inflammation and immunity. Trends Immunol. 2011; 32:335–43. [PubMed: 21570914]
36. Sopel MJ, Rosin NL, Lee TD, Legare JF. Myocardial fibrosis in response to Angiotensin II is preceded by the recruitment of mesenchymal progenitor cells. Lab Invest. 2011; 91:565–78. [PubMed: 21116240]
37. Lagger G, O'Carroll D, Rembold M, Khier H, Tischler J, Weitzer G, et al. Essential function of histone deacetylase 1 in proliferation control and CDK inhibitor repression. EMBO J. 2002; 21:2672–81. [PubMed: 12032080]
38. Sambucetti LC, Fischer DD, Zabludoff S, Kwon PO, Chamberlin H, Trogani N, et al. Histone deacetylase inhibition selectively alters the activity and expression of cell cycle proteins leading to specific chromatin acetylation and antiproliferative effects. J Biol Chem. 1999; 274:34940–7. [PubMed: 10574969]
39. Shao DD, Suresh R, Vakil V, Gomer RH, Pilling D. Pivotal Advance: Th-1 cytokines inhibit, and Th-2 cytokines promote fibrocyte differentiation. J Leukoc Biol. 2008; 83:1323–33. [PubMed: 18332234]
40. Duffield JS, Lupher ML Jr. PRM-151 (recombinant human serum amyloid P/pentraxin 2) for the treatment of fibrosis. Drug News Perspect. 2010; 23:305–15. [PubMed: 20603654]

41. Gui CY, Ngo L, Xu WS, Richon VM, Marks PA. Histone deacetylase (HDAC) inhibitor activation of p21WAF1 involves changes in promoter-associated proteins, including HDAC1. Proc Natl Acad Sci U S A. 2004; 101:1241–6. [PubMed: 14734806]
42. Li H, Wu X. Histone deacetylase inhibitor, Trichostatin A, activates p21WAF1/CIP1 expression through downregulation of c-myc and release of the repression of c-myc from the promoter in human cervical cancer cells. Biochem Biophys Res Commun. 2004; 324:860–7. [PubMed: 15474507]
43. Marks PA. The clinical development of histone deacetylase inhibitors as targeted anticancer drugs. Expert Opin Investig Drugs. 2010; 19:1049–66.
44. Richon VM, Sandhoff TW, Rifkind RA, Marks PA. Histone deacetylase inhibitor selectively induces p21WAF1 expression and gene-associated histone acetylation. Proc Natl Acad Sci U S A. 2000; 97:10014–9. [PubMed: 10954755]
45. Wynn TA, Barron L. Macrophages: master regulators of inflammation and fibrosis. Semin Liver Dis. 2010; 30:245–57. [PubMed: 20665377]
46. Dinarello CA, Fossati G, Mascagni P. Histone deacetylase inhibitors for treating a spectrum of diseases not related to cancer. Mol Med. 2011; 17:333–52. [PubMed: 21556484]
47. Leoni F, Fossati G, Lewis EC, Lee JK, Porro G, Pagani P, et al. The histone deacetylase inhibitor ITF2357 reduces production of pro-inflammatory cytokines in vitro and systemic inflammation in vivo. Mol Med. 2005; 11:1–15. [PubMed: 16557334]
48. McKinsey TA. Targeting inflammation in heart failure with histone deacetylase inhibitors. Mol Med. 2011; 17:434–41. [PubMed: 21267510]
49. Duerrschmid C, Crawford JR, Reineke E, Taffet GE, Trial J, Entman ML, et al. TNF receptor 1 signaling is critically involved in mediating angiotensin-II-induced cardiac fibrosis. J Mol Cell Cardiol. 2013
50. Nikam VS, Wecker G, Schermuly R, Rapp U, Szelepusa K, Seeger W, et al. Treprostinil inhibits the adhesion and differentiation of fibrocytes via the cyclic adenosine monophosphate-dependent and Ras-proximate protein-dependent inactivation of extracellular regulated kinase. Am J Respir Cell Mol Biol. 2011; 45:692–703. [PubMed: 21278326]
51. Haudek SB, Gupta D, Dewald O, Schwartz RJ, Wei L, Trial J, et al. Rho kinase-1 mediates cardiac fibrosis by regulating fibroblast precursor cell differentiation. Cardiovasc Res. 2009; 83:511–8. [PubMed: 19406912]
52. Kokubo S, Sakai N, Furuichi K, Toyama T, Kitajima S, Okumura T, et al. Activation of p38 mitogen-activated protein kinase promotes peritoneal fibrosis by regulating fibrocytes. Perit Dial Int. 2012; 32:10–9. [PubMed: 21719683]
53. Ferguson BS, Harrison BC, Jeong MY, Reid BG, Wempe MF, Wagner FF, et al. Signal-dependent repression of DUSP5 by class I HDACs controls nuclear ERK activity and cardiomyocyte hypertrophy. Proc Natl Acad Sci U S A. 2013; 110:9806–11. [PubMed: 23720316]
54. Galligan CL, Siminovitch KA, Keystone EC, Bykerk V, Perez OD, Fish EN. Fibrocyte activation in rheumatoid arthritis. Rheumatology (Oxford). 2010; 49:640–51. [PubMed: 19858121]
55. Moeller A, Gilpin SE, Ask K, Cox G, Cook D, Gauldie J, et al. Circulating fibrocytes are an indicator of poor prognosis in idiopathic pulmonary fibrosis. Am J Respir Crit Care Med. 2009; 179:588–94. [PubMed: 19151190]
56. Gomperts BN, Strieter RM. Fibrocytes in lung disease. J Leukoc Biol. 2007; 82:449–56. [PubMed: 17550974]
57. Frid MG, Brunetti JA, Burke DL, Carpenter TC, Davie NJ, Reeves JT, et al. Hypoxia-induced pulmonary vascular remodeling requires recruitment of circulating mesenchymal precursors of a monocyte/macrophage lineage. Am J Pathol. 2006; 168:659–69. [PubMed: 16436679]
58. Yeager ME, Nguyen CM, Belchenko DD, Colvin KL, Takatsuki S, Ivy DD, et al. Circulating fibrocytes are increased in children and young adults with pulmonary hypertension. Eur Respir J. 2012; 39:104–11. [PubMed: 21700605]
59. Phillips RJ, Burdick MD, Hong K, Lutz MA, Murray LA, Xue YY, et al. Circulating fibrocytes traffic to the lungs in response to CXCL12 and mediate fibrosis. J Clin Invest. 2004; 114:438–46. [PubMed: 15286810]

60. Wu GD, Nolta JA, Jin YS, Barr ML, Yu H, Starnes VA, et al. Migration of mesenchymal stem cells to heart allografts during chronic rejection. Transplantation. 2003; 75

61. Wada T, Sakai N, Sakai Y, Matsushima K, Kaneko S, Furuichi K. Involvement of bone-marrow-derived cells in kidney fibrosis. Clin Exp Nephrol. 2011; 15:8–13. [PubMed: 21152947]

62. Scholten D, Reichart D, Paik YH, Lindert J, Bhattacharya J, Glass CK, et al. Migration of fibrocytes in fibrogenic liver injury. Am J Pathol. 2011; 179:189–98. [PubMed: 21703401]

63. Liu N, He S, Ma L, Ponnusamy M, Tang J, Tolbert E, et al. Blocking the class I histone deacetylase ameliorates renal fibrosis and inhibits renal fibroblast activation via modulating TGF-beta and EGFR signaling. PLoS One. 2013; 8:e54001. [PubMed: 23342059]

64. Borbely A, vand V, Papp Z, Bronzwaer JG, Edes I, Stienen GJ, et al. Cardiomyocyte stiffness in diastolic heart failure. Circulation. 2005; 111:774–81. [PubMed: 15699264]

65. Hamdani N, Paulus WJ. Myocardial titin and collagen in cardiac diastolic dysfunction: partners in crime. Circulation. 2013; 128:5–8. [PubMed: 23709670]

66. Janicki JS, Brower GL. The role of myocardial fibrillar collagen in ventricular remodeling and function. J Card Fail. 2002; 8:S319–S325. [PubMed: 12555139]

67. Wu Y, Cazorla O, Labeit D, Labeit S, Granzier H. Changes in titin and collagen underlie diastolic stiffness diversity of cardiac muscle. J Mol Cell Cardiol. 2000; 32:2151–62. [PubMed: 11112991]

68. Owan TE, Hodge DO, Herges RM, Jacobsen SJ, Roger VL, Redfield MM. Trends in prevalence and outcome of heart failure with preserved ejection fraction. N Engl J Med. 2006; 355:251–9. [PubMed: 16855265]

69. Roger VL, Go AS, Lloyd-Jones DM, Adams RJ, Berry JD, Brown TM, et al. Heart disease and stroke statistics--2011 update: a report from the American Heart Association. Circulation. 2011; 123:e18–e209. [PubMed: 21160056]

70. Boumber Y, Younes A, Garcia-Manero G. Mocetinostat (MGCD0103): a review of an isotype-specific histone deacetylase inhibitor. Expert Opin Investig Drugs. 2011; 20:823–9.

71. Niu J, Kolattukudy PE. Role of MCP-1 in cardiovascular disease: molecular mechanisms and clinical implications. Clin Sci (Lond). 2009; 117:95–109. [PubMed: 19566488]

72. McKinsey TA. Isoform-selective HDAC inhibitors: closing in on translational medicine for the heart. J Mol Cell Cardiol. 2011; 51:491–6. [PubMed: 21108947]

Appendix A. Supplementary Material

sFig. 1. α-Smooth muscle actin expression in cultured cardiac myocytes. Primary adult rat ventricular fibroblasts (ARVFs) were isolated as described in the Materials and methods section. Protein homogenates were immunoblotted to detect α-smooth muscle actin expression as a marker of myofibroblast differentiation. Calnexin served as a loading control. Passage 0 = cells isolated from hearts and lysed prior to culture.

sFig. 2. HDAC inhibitor selectivity in live cardiac fibroblasts. Cultured adult rat ventricular fibroblasts were treated for 24 hours with increasing concentrations of the indicated HDAC inhibitors and then exposed to cell-permeable, fluorogenic HDAC substrates for 20 minutes. Half maximal inhibitor concentrations (IC_{50s}) are shown for each compound.

sFig. 3. Characterization of cardiac hypertrophy and function in Ang II treated mice. (A) Two weeks of Ang II treatment, as described in Fig. 1, failed to induce significant left ventricular (LV) hypertrophy. Diastolic LV function was preserved in Ang II-treated mice, as determined by pulsed-wave Doppler measurements of mitral inflow velocities (B) and tissue Doppler to quantify septal mitral annulus velocities (C). (D) M-mode echocardiography measurements failed to reveal significant systolic LV dysfunction in Ang II-treated mice. IVS = interventricular septum; LVPW = left ventricular posterior wall.

sFig. 4. Class I HDAC inhibition blocks Ang II-mediated cardiac fibrosis. The images shown in Fig. 2 were captured at 2.5X magnification to reveal the overall level of LV fibrosis, as determined by picrosirius red dye staining of interstitial collagen. Scale bar = 10 μm.

sFig. 5. Class I HDAC isoforms are expressed in the mouse LV. Expression levels of class I HDACs -1, -2 and -3 were assessed by immunoblotting of protein in mouse LV homogenates. Each class I HDAC isoform was detected in the LV, and levels of the proteins were not altered by two weeks of Ang II treatment. Calnexin served as a loading control.

sFig. 6. Inhibition of class I HDACs reduces circulating fibrocyte numbers. Representative graphs of circulating fibrocytes, defined as $CD45^+CD34^+$ and αSMA^+ or Col I^+ cells, from mice infused with Ang II for three days in the absence or presence of MGCD0103. Quantification is shown in Fig. 6D.

sFig. 7. Intracellular staining controls for flow cytometry. Based on IgG (isotype) controls, gates were set to differentiate between fluorescent positive and fluorescent negative cell populations for each channel. (A) Intracellular and IgG control staining of fixed and permeabilized $CD45^+CD34^+$FSC/SSC-gated cells identified in single cell suspensions of pooled LVs from mice treated for three days with Ang II; these are the controls for the data shown in Fig. 6B. (B) IgG control staining of fixed and permeabilized FSC/SSC-gated cells identified in blood pooled from each animal across the three treatment groups; this is a control for the data shown in Fig. 6D. (C) IgG control staining of fixed and permeabilized human peripheral blood mononuclear cells (PBMCs) that were cultured and stimulated with IL-4 and IL-13 for five days; this is a control for the data shown in Fig. 7A.

sFig. 8. MGCD0103 stimulates MCP-1 expression in cultured cardiac fibroblasts. Adult rat ventricular fibroblasts (ARVFs) were cultured in serum-free medium and stimulated with Ang II (10 μM) in the absence or presence of MGCD0103 (300 nM) for 24 hours. Total RNA was isolated and MCP-1 mRNA expression was quantified by qRT-PCR (left-hand panel). A second experiment was performed with ARVFs isolated on a separate day and treated with MGCD0103 alone for 24 hours (right-hand panel). N = 3 plates of cells per condition. Data represent means +SEM; $*P < 0.05$ vs. untreated, DMSO control. The data indicate that MGCD0103 alone is capable of stimulating MCP-1 mRNA expression.

sTable 1. Primer sequences for quantitative PCR.

Highlights

- Selective pharmacological inhibition of class I HDACs blocks cardiac fibrosis
- Class I HDAC inhibition blocks differentiation of bone marrow-derived cells into fibrocytes, which contribute to diverse fibrotic processes
- Class I HDAC inhibition blocks cardiac fibroblast activation

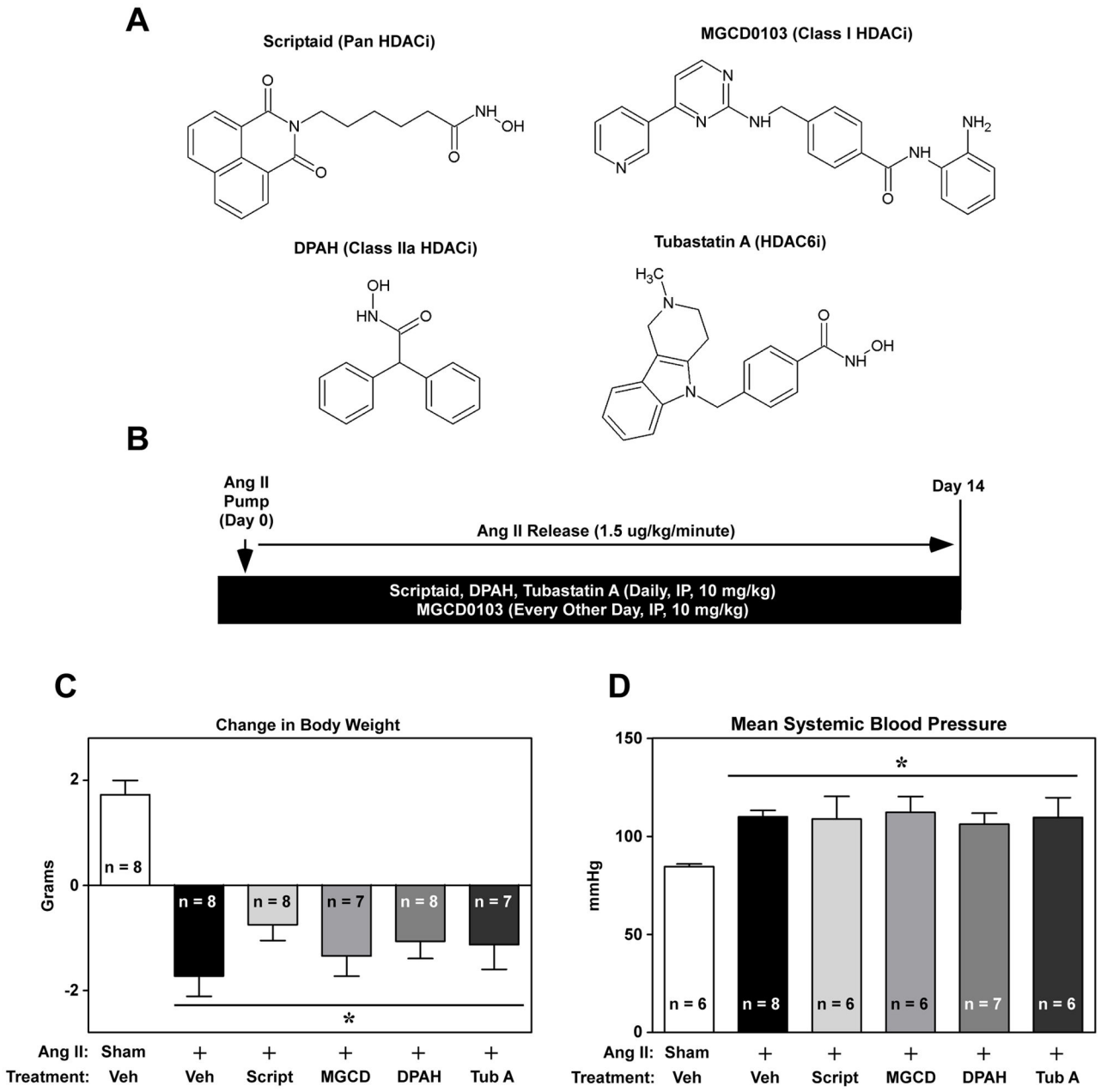

Fig. 1.

Isoform-selective HDAC inhibition in a mouse model of Ang II-mediated cardiac fibrosis. (A) Structures and selectivity profiles of the small molecule HDAC inhibitors used *in vivo*. (B) Scriptaid, DPAH, Tubastatin A were dosed IP at 10 mg/kg daily. Due to the slow on/off-rate of MGCD0103 (MGCD), dosing with this class I inhibitor was alternated every other day with vehicle injections. HDAC inhibitor treatment began at the time of angiotensin II (Ang II) mini-pump implantation. (C) Animal body weight was measured at the beginning of the study and immediately prior to animal sacrifice on day 14 of the study. (D) Systemic blood pressure was determined in anesthetized animals with a catheter placed in the common carotid artery. Data represent means + SEM; **P* < 0.05 vs. sham + vehicle control.

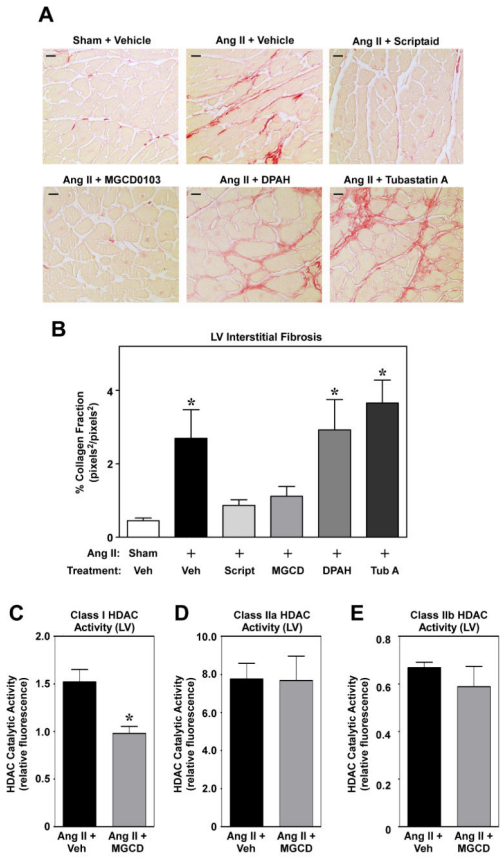

Fig. 2.

Class I HDAC-selective inhibition prevents Ang II-mediated cardiac fibrosis. (A) Representative images (40X magnification) of LV sections stained with picrosirius red for interstitial collagen; LVs were obtained from mice treated with Ang II in the absence or presence of HDAC inhibitors for 14 days. Scale bar = 10 μm. (B) Quantification of picrosirius red staining was completed by determining the average stained pixels^2 per total pixels^2 in images of the LV using AxioVision software (18 investigator-blinded images used per animal; n = 7 – 8 animals/group). Data represent means + SEM; *P< 0.05 vs. sham + vehicle control. (C – E) HDAC enzymatic activity assays were performed using LV homogenates from mice treated with Ang II in the absence or presence of MGCD0103; n = 4 per group. Enzyme activity was normalized to α-tubulin expression, as assessed by immunoblotting. Data represent means + SEM; *P < 0.05 vs. Ang II + vehicle.

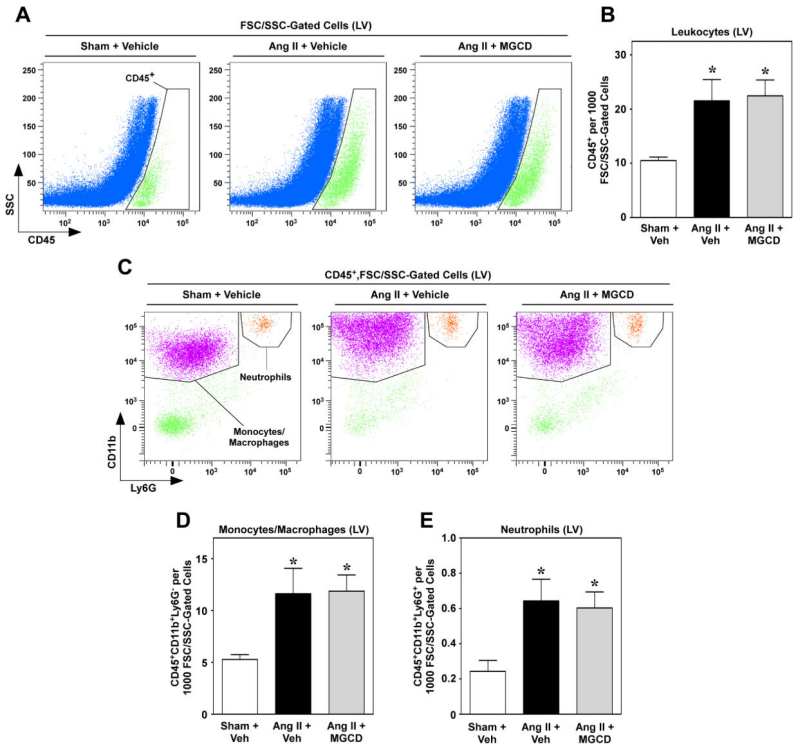

Fig. 3.

Class I HDAC inhibition does not reduce leukocyte recruitment to the heart. Representative flow cytometric dot plots of cardiac LV single-cell suspensions taken from mice treated as indicated for three days. Cells were first gated on FSC/SSC properties to exclude the majority of debris and dead cells. (A) Cells falling within the FSC/SSC gate were analyzed for $CD45^+$ positivity against SSC. (B) Quantification of $CD45^+$ cells in mouse LV; n = 8/group. (C) $CD45^+$ cells were then further analyzed for expression of CD11b and Ly6G to identify the monocyte/macrophage and neutrophil populations. (D and E) Quantification of indicated populations of monocytes/macrophages ($CD45^+CD11b^+Ly6G^-$) and neutrophils ($CD45^+CD11b^+Ly6G^+$) in LV single-cell suspensions; n = 8/group. Data for (B), (D) and (E) represent means +SEM; $*P < 0.05$ vs. sham + vehicle control.

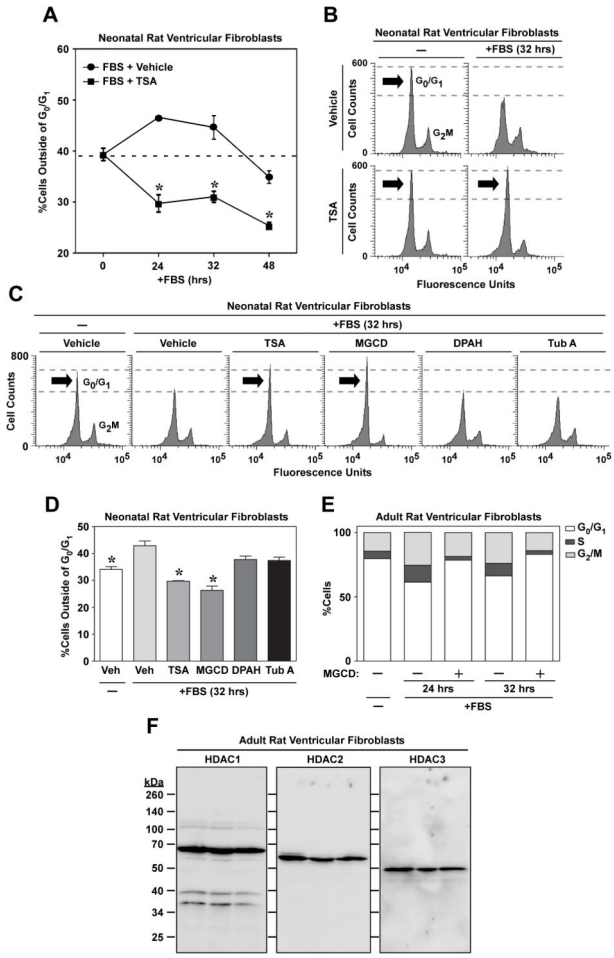

Fig. 4.

Class I HDAC inhibition arrests cardiac fibroblast cell cycle progression. (A) Cultured neonatal rat ventricular fibroblasts were synchronized and then stimulated with FBS (20%) in the absence or presence of the pan-HDAC inhibitor, trichostatin A (TSA). At the indicated times post-FBS treatment, cells were stained with propidium iodide and cell cycle progression analyzed by flow cytometry; n = 3 plates of cells/condition. Data represent means +/− SEM; **P* < 0.05 vs. FBS + vehicle. (B) Representative histograms of propidium iodide-stained cells. (C) Cells were stimulated for 32 hours with FBS in the absence or presence of the indicated HDAC inhibitors. (D) Quantification of cells outside of G_0/G_1; n = 3 plates of cells/condition. Data represent means + SEM; **P* < 0.05 vs. FBS + vehicle. (E) Adult rat ventricular fibroblasts (ARVFs) were stimulated with FBS for 24 or 32 hrs in the absence or presence of MGCD0103 (MGCD; 1 μM). Average number of cells in G_0/G_1, S or G_2M phases of the cell cycle was quantified by flow cytometry; n = 3 plates of cells/condition. (F) Lysates were prepared from three independent plates of unstimulated ARVFs and immunoblotting was performed to assess expression of HDAC1, HDAC2 and HDAC3 protein.

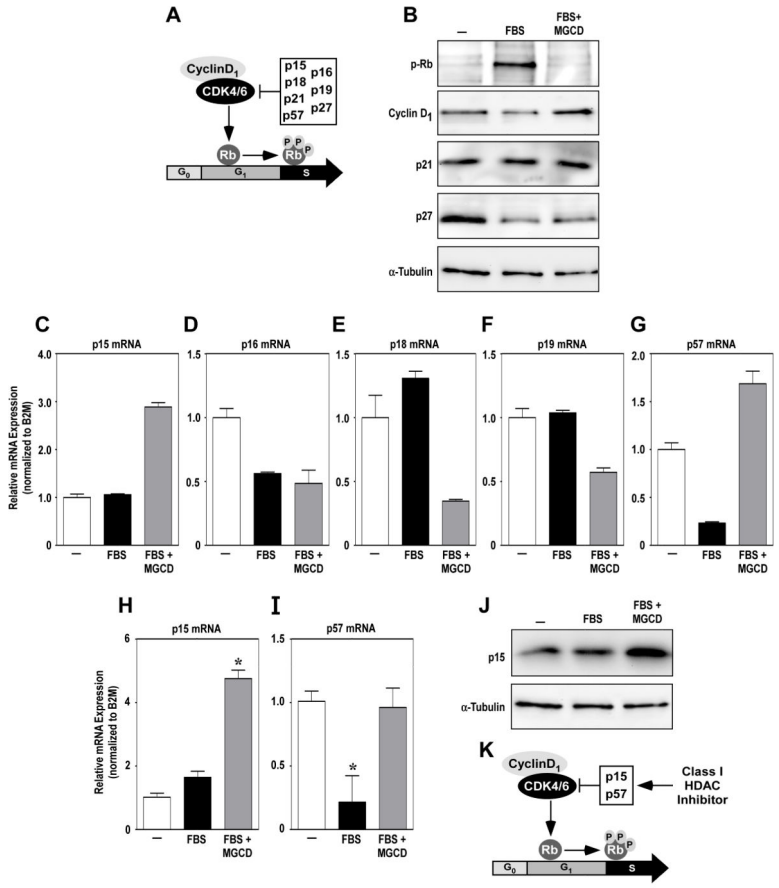

Fig. 5.

Class I HDAC inhibition stimulates p15 and p57 expression in cardiac fibroblasts. (A) Cyclin-dependent kinase (CDK) inhibitors p15, p16, p18, p21, p27, and p57 inhibit the activity of the Cyclin D_1/CDK4/6 complexes, preventing the phosphorylation of Rb and progression to the S phase of the cell cycle. (B) Immunoblotting was performed with homogenates from neonatal rat ventricular fibroblasts (NRVFs) treated for 32 hours with FBS in the absence or presence of the class I HDAC inhibitor, MGCD0103. (C – G) Quantitative reverse transcriptase PCR (qRT-PCR) was performed with RNA from NRVFs stimulated for 32 hours with FBS in the absence or presence of MGCD0103. RNA was pooled from 4 plates of cells/condition; qRT-PCR was performed with duplicate samples and averages are shown. Error bars represent SEM from technical duplicates. (H and I) Follow-up qRT-PCR studies were performed with RNA from three independent plates of NRVFs treated as indicated. *$P < 0.05$ vs. unstimulated control. (J) Immunoblot analysis of NRVF lysates was performed with an anti-p15 antibody. (K) Data suggest that class I HDAC inhibition blocks cardiac fibroblast cell cycle progress, in part, via induction of p15 and p57.

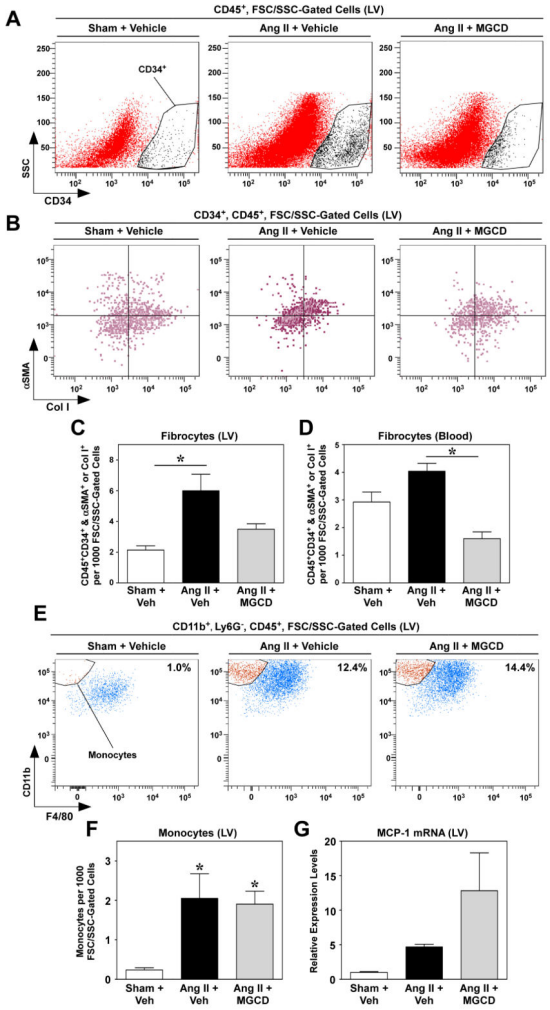

Fig. 6.

Class I HDAC inhibition reduces fibrocyte numbers in the heart and in circulation. (A) Single-cell suspensions derived from LVs of mice treated as indicated for three days. For all analyses, initial gating was on FSC/SSC properties to exclude the majority of debris and dead cells. Cells staining positive for CD45 were analyzed for co-expression of CD34. Representative flow cytometric dot plots of $CD34^+$ cells (within the $CD45^+$ gate) against SSC are shown. (B) This putative fibrocyte population ($CD34^+CD45^+$) was further analyzed for expression of either αSMA or Col I to define fibrocytes. Quantification of fibrocyte populations in the LV (C) and in circulation (D) at the end of the three day study; n = 4 animals/group. Data represent means +SEM; $*P < 0.05$. (E) To determine if there were differences in the percentage of monocytes, single-cell suspensions of LV were analyzed for CD45 positivity. Cells staining positive for CD45 were analyzed for co-expression of CD11b. $CD45^+CD11b^+$ cells were then analyzed for Ly6G expression and a gate was set to select $Ly6G^-$ cells (within the $CD45^+CD11b^+$ population), so as to exclude neutrophils. To identify monocytes, cells within the $CD45^+CD11b^+Ly6G^-$ population were analyzed for F4/80 positivity and monocytes were defined as those cells staining negative for the macrophage marker F4/80. Representative flow cytometric dot plot images of

$CD45^{+}CD11b^{+}Ly6G^{-}$ cells being analyzed for F4/80 positivity against CD11b are shown. (F) Monocyte numbers in the LV were quantified. Data represent means +SEM; n = 8 animals/group. (G) Quantitative reverse transcriptase PCR was performed with LV RNA to measure monocyte chemoattractant protein-1 (MCP-1) mRNA levels.

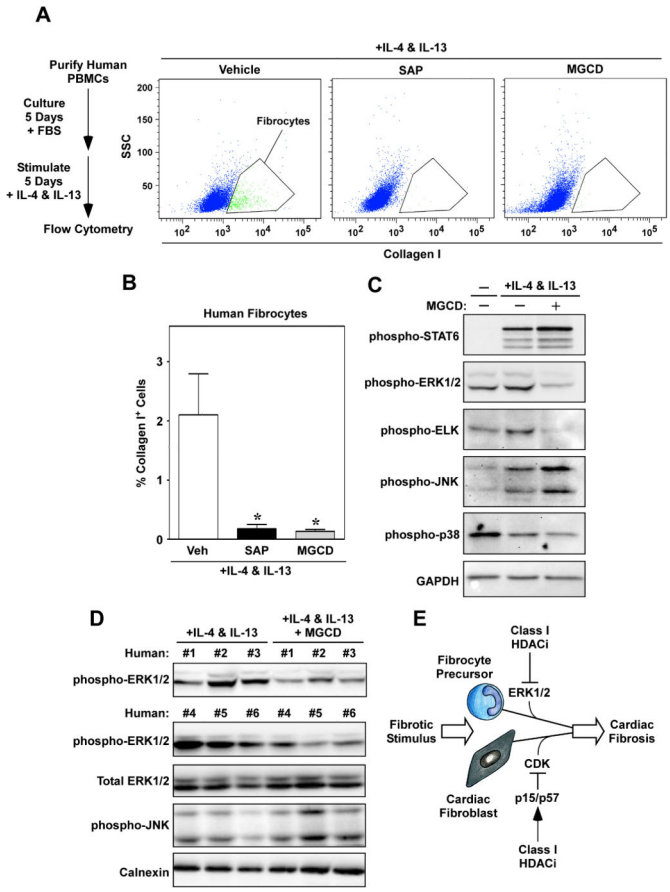

Fig. 7.

Class I HDAC inhibition blocks fibrocyte differentiation. (A) Circulating peripheral blood mononuclear cells (PBMCs) were purified from human whole blood and cultured for five days prior to stimulation with IL-4 and IL-13 in serum-free differentiation medium for an additional five days. Some cells received the class I HDAC inhibitor, MGCD0103 (MGCD; 250 nM), or serum amyloid P (SAP; 1 μg/ml). Shown are representative graphs of collagen I-positive cells identified using flow cytometry. (B) Collagen I-positive cells were quantified. **P* < 0.05 vs. IL-4 & IL-13 + vehicle; n = 4/condition. (C) Whole cell lysates from cells treated with IL-4 and IL-13 in the absence or presence of MGCD were subjected to immunoblotting with the indicated antibodies; lysates from 5 plates of cells per condition were pooled in order to obtain enough protein for biochemical characterization. (D) To confirm the findings shown in (C), PBMCs from six individuals were treated with IL-4 and IL-13 in the absence or presence of MGCD. The data illustrate consistent suppression of ERK1/2 phosphorylation in class I HDAC inhibitor-treated cells, and no effect of MGCD on total ERK levels or JNK phosphorylation. (E) A model for regulation of cardiac fibrosis by class I HDACs.